JOURNAL OF THERMOPHYSICS AND HEAT TRANSFER
Vol. 14, No. 4, October–December 2000

Two-Dimensional Ablation in Cylindrical Geometry

Subrahmanya S. Katte,* S. K. Das,† and S. P. Venkateshan‡
Indian Institute of Technology, Madras, Chennai 600 036, India

Ablation modeling in cylindrical geometry is a very important problem in the thermal modeling of spacecraft, which has not been dealt with adequately in the literature. In the present work, two-dimensional ablation in cylindrical geometry is considered when the incident heat flux varies axially as well as temporally. A novel idea of using an effective inverse Stefan number, which is analogous to the effective heat of ablation (used in the literature), is proposed to be used as a variable nondimensional latent heat of ablation for ablation modeling, indirectly accounting for various processes involved in ablation. A two-dimensional ablation problem is solved by an alternating direction implicit and adjustable time-step scheme, coupled with boundary immobilization. Quasi-one-dimensional and two-dimensional modeling methods have been compared for two different materials, and the effects of variation of the proposed inverse Stefan number with the incident heat flux and the presence of highly conducting structure bonded to the ablative material have been studied. An optimum modeling method under specific conditions is suggested.

Nomenclature

C_1, C_2	=	constants; Eq. (17)
c_p	=	specific heat, J/kg K
D	=	domain of the ablative material
$f(r, z, t)$	=	function describing the ablation front
H_{eff}	=	effective heat of ablation, $q/(\rho s)$, J/kg
k	=	thermal conductivity, W/m K
L	=	latent heat of ablation, J/kg
l	=	length of the cylinder, m
$\hat{n}$	=	outward surface normal at any location
$q(z, t)$	=	incident heat flux, function of axial coordinate and time, W/m^2
r, z	=	radial and the axial coordinates in cylindrical coordinate system, respectively, m
$r_\delta(z, t)$	=	local radius of the ablation front, function of axial coordinate and time, m
s	=	local recession rate of ablation front, $\partial\delta/\partial t$, m/s
T	=	temperature, K
t	=	time, s
X	=	original thickness of the ablative material, $(r_o - r_i)$, m
α	=	thermal diffusivity in the constant thermal conductivity model, m^2/s
$\Delta r, \Delta z$	=	grid sizes in radial and axial directions, respectively, m
ΔT	=	temperature margin used for the adjustable time step numerical scheme, K
Δt	=	time step, s
$\delta(z, t)$	=	local ablated material thickness, m
$\eta(r, \delta)$	=	Landau-type transformed variable, $(r - r_i)/\{r_o - r_i - \delta(z, t)\}$
ν	=	inverse Stefan number, $L/\{c_p(T_p - T_0)\}$
ρ	=	density of virgin material, kg/m^3

Subscripts

avg	=	average
eff	=	effective
i, o	=	inside and outside, respectively
n	=	normal component
net	=	net
p	=	onset of ablation
r	=	radial component
s	=	cylindrical structure
0	=	initial

Superscripts

l	=	current time level
$l - \frac{1}{2}$	=	half time step before current time level
$l + \frac{1}{2}$	=	half time step after current time level
$l + 1$	=	one time step after current time level

Introduction

THERMAL design and analysis of spacecraft structures and thermal protection system (TPS) assemblies form an important part of the design and development cycle for both launch and reentry vehicles. This involves modeling of the ablation problem in cylindrical geometry, for a range of low-ablation insulating materials (composites) to high-ablation (carbonaceous) materials. A severe heat flux, which varies with time as well as location, acts on the ablative material, which is initially in its virgin phase. As the temperature rises, it can experience one or several transformations, typically pyrolysis, oxidation, and melting or sublimation, depending on the incident heat flux variation and the material characteristics. Because of its thermochemical nature, ablation modeling of composite materials accounting for all intermediate transformations is an arduous task. Also, the regimes and rate of these intermediate transformations strongly depend on the magnitude and the nature of temporal variation of the incident heat flux at a given location. This is because the oxidation rate, mechanism of heat rejection by reradiation, and melting or sublimation depends on the magnitude, whereas pyrolysis depends on the nature of temporal variation of the incident heat flux. Furthermore, with the spatial variation of the incident heat flux, not only the effect of multidimensionality on heat transfer will come into picture, but also different transformations will be taking place at different locations at the same time. Ablation modeling of a spacecraft TPS accounting for all intermediate transformations thus becomes a major challenge.

Because of its practical importance, the ablation problem has received considerable attention. One-dimensional planar ablation has been studied analytically by Landau.[1] Analytical approximate methods such as heat balance integral and variational methods were introduced by several workers[2–4] to treat the nonlinear nature of the governing equations for planar one-dimensional ablation, especially

Received 7 January 2000; revision received 27 April 2000; accepted for publication 2 May 2000.

*Research Scholar, Department of Mechanical Engineering, permanently Lecturer in Mechanical Engineering, Shanmugha College of Engineering, Tirumalaisamudram, 613 402 India.
†Assistant Professor, Department of Mechanical Engineering.
‡Professor, Heat Transfer and Thermal Power Laboratory, Department of Mechanical Engineering; spv46@usa.net.

when the incident heat flux is time dependent. Because the choice of the approximate profile determines the accuracy of the solution in using cited methods, the general integral method was introduced by Venkateshan and Solaiappan,[5] in which the general integral relation is independent of the choice of the profile. Ledder[6] reduced the planar steady one-dimensional ablation problem to a single Volterra integral equation by the spatial Laplace transform method. An inverse problem of planar one-dimensional nonlinear heat conduction with surface ablation to recover the time-dependent heat flux and surface recession history has been considered recently.[7]

One-dimensional ablation in cylindrical coordinates using Landau[1] transformation and a finite control volume procedure was considered recently by Blackwell and Hogan.[8] Because the spherical geometry is applicable to ablation at nose cone of a reentry vehicle, two-dimensional ablation of a sphere has been considered[9] by application of a novel deforming finite element technique. Ablation of a spherical body was numerically modeled as two-phase Stefan problem[10] through a fixed domain numerical scheme based on the enthalpy formulation. Hogan et al.[11] applied a moving grid control volume finite element method to the two-dimensional axisymmetric ablation problem with unstructured grids and presented the practical application of this approach to the ablation of a reentry vehicle nose tip. Ablation modeling of composite materials, too, has received some attention. A one-dimensional material thermal response model for newly developed composite phenolic impregnated carbon ablators has been reported[12] along with the experimental results for other traditionally used materials such as carbon and Avcoat®. Surface recession and mass loss correlations were developed for reinforced carbon–carbon composite through thermal testing to determine its oxidation characteristics.[13]

It appears that two-dimensional ablation in cylindrical geometry has not been addressed in the literature even though it is important in the thermal modeling of reentry and launch vehicles, where the surface heat flux varies spatially as well as temporally. There are no indications available in the literature to suggest an optimum and efficient modeling method for ablation problem in spacecraft TPS design. The present study addresses the problem of two-dimensional ablation in cylindrical geometry. A novel idea for ablation modeling for spacecraft applications is proposed without considering complex chemical reactions, nonetheless indirectly accounting for all intermediate transformations of the composite material through the use of an effective inverse Stefan number, when the incident heat flux is a function of location as well as time. For representative cases and two different materials, the two-dimensional model is compared with the quasi-one-dimensional model. The effect of variation of the proposed effective inverse Stefan number with the incident heat flux and the effect of presence of highly conducting structure when the ablative material is bonded to it are studied to suggest an optimum and efficient modeling method for spacecraft TPS design applications.

Effective Inverse Stefan Number Model Proposed for Composites

A novel idea for ablation modeling of composite materials is proposed to account for the intermediate transformations. The effective heat of ablation H_{eff}, which is generally used to evaluate the performance of ablative materials, is the heat absorbed per unit mass normalized to the virgin density and is a function of incident heat flux itself. For a given material and for a given incident heat flux H_{eff} can be obtained from experimental databases, and the corresponding value of the proposed effective inverse Stefan number ν_{eff} can be found by solving an inverse problem. For a given incident heat flux q and for a particular value of inverse Stefan number ν, the surface recession rate s is obtained by solving the planar one-dimensional ablation problem, which is used to evaluate the effective heat of ablation $H_{\text{eff}} = q/(\rho s)$. This procedure is repeated, and H_{eff} for the given incident heat flux is evaluated as a function of ν over a range of interest. It is found that H_{eff} thus evaluated increases linearly with ν for a given incident heat flux, and ν_{eff} corresponding to the experimental value of H_{eff} can be obtained by this straight line fit. The ν_{eff} thus obtained is interpreted as an effective inverse Stefan number of the composite for the given incident heat flux and is analogous to H_{eff}, which includes implicitly the effect of all intermediate transformations.

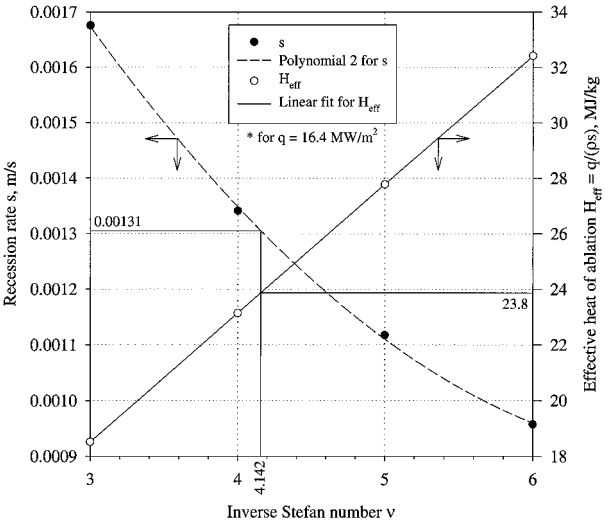

Fig. 1 Effective heat of ablation and recession rate variation with inverse Stefan number.

The described procedure of obtaining ν_{eff} is repeated for discrete values of incident heat flux over a range representative of launch and entry conditions, for which H_{eff} data based on experiments are known. Now the variation of ν_{eff} with incident heat flux q is expressed in the form of a polynomial of appropriate degree, which can be used for further modeling. Hence, any spacecraft TPS ablation problem can be treated as Stefan-type ablation for all composite materials. The effective inverse Stefan number, which is a function of incident heat flux itself, is used as the non-dimensional latent heat of ablation in this model, whose instantaneous and local value is obtained from the preceding polynomial relationship. If the specific heat of the ablative material is a function of temperature, it is evaluated at ablation temperature T_p while ν_{eff} is interpreted. The effects of multidimensionality and intermediate transformations can be easily handled in this way, by utilizing ν_{eff} as variable material property data even when the incident heat flux varies spatially as well as temporally. Because H_{eff} data are based on experiments, the proposed ν_{eff} method of ablation modeling can be termed as a semi-empirical method.

The preceding procedure is demonstrated for the ablative material Avcoat 5026 H/CG for an incident heat flux range of 2.27–16.4 MW/m^2 representative of reentry conditions; the effective heat of ablation along with other properties based on experimental results have been presented in a NASA Ames Research Center material database.[14] A 50-mm-thick, one-dimensional slab with an insulated boundary condition at the other end was considered for this case, with a grid size of 0.1 mm, chosen based on a grid independence study. It was assumed that the ablative material, which is initially at a uniform temperature of 300 K, reradiates to an ambient at 300 K, and the given heat flux is applied at $t = 0$. The resultant system of equations was solved iteratively by a semi-implicit finite difference scheme, after immobilizing the boundary through Landau[1] transformation. Figure 1 shows the variations of both surface recession rate at $t = 10$ s and H_{eff} with ν, obtained by the described procedure for an incident heat flux of 16.4 MW/m^2. For an incident heat flux of 16.4 MW/m^2, Ref. 14 gives an H_{eff} of 23.8 MJ/kg based on experiments, and the corresponding ν_{eff} was found to be 4.142. When the problem is treated as Stefan-type ablation, an equivalent surface recession rate of 1.31 mm/s is obtained by extending the ν_{eff} line as seen.

Figure 2 shows the variation of ν_{eff} obtained by the described procedure in the form of a polynomial of degree 4, the variation of H_{eff} as given by the NASA Ames Research Center material database,[14] and the resultant surface recession rate variation at $t = 10$ s with the incident heat flux q. It can be seen that the rate of increase in the

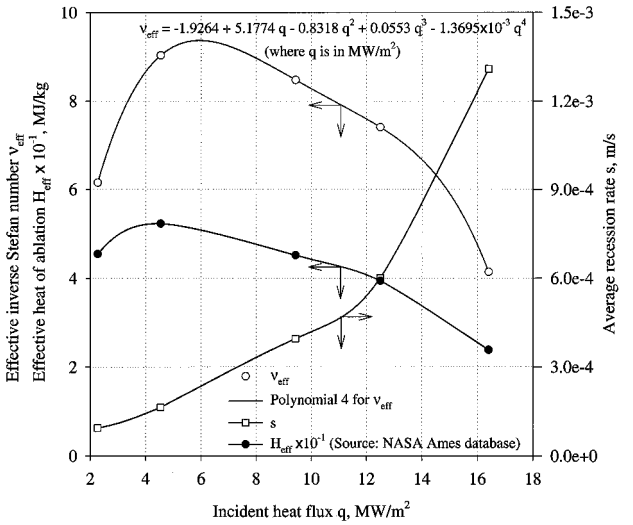

Fig. 2 Variation of effective inverse Stefan number and recession rate with incident heat flux.

surface recession rate is relatively higher at higher values of incident heat flux because the melting or sublimation becomes severe with further increase in q. At heating rates above 2.27 MW/m^2 up to about 5 MW/m^2, the ablation characteristic is diffusion controlled, and the main mechanism of heat rejection is reradiation. The material becomes more efficient with increasing heat flux over this range and is evident by the increasing trend in H_{eff}. The second regime, melting or sublimation rate controlled, occurs at heating rates above 5 MW/m^2, where the surface recession is primarily due to melting or sublimation, thus contributing to high recession and, thus, resulting in a reduction in the resultant H_{eff} with increase in q. The variation of v_{eff} with the incident heat flux follows the same trend because it is analogous to H_{eff}, and its variation is quite significant over the range considered. In what follows, the v_{eff} concept is used for ablation modeling for the Avcoat material.

Two-Dimensional Ablation: Mathematical Modeling

Consider a metallic cylindrical structure, with an ablative material of uniform original thickness X bonded to it as shown in Fig. 3a, with insulated boundary condition at both ends. The ablative material is initially at a uniform temperature of T_0, less than the ablation temperature T_p, and the surface of the cylinder, which reradiates to an ambient at 300 K, is subjected to a given heat flux $q(z, t)$. The interior surface of the ablative material can have either an insulated boundary condition or a highly conducting metallic structure attached to it without any contact resistance. The interior surface of the metallic structure, which has a thickness of $(r_i - r_s)$, is assumed to be insulated in the latter case.

Initially the material occupies the domain $(r_o - r_i)$ with the outer boundary at $r = r_o$. Because of the thermal load, the temperature rises, and once the ablation temperature T_p is reached at some time $t = t_p$ at some point of the boundary, the material begins to be removed. This period from $t = 0$ to t_p is referred to as the preablation period. As the heating continues, ablation commences with the ablation front progressing into the solid, and this period is referred to as the ablation period. It is assumed that the ablated material is removed instantaneously and completely on its formation, so that the ablation front acts as a new (moving) boundary on which the external heat flux acts. For the ablation period $t > t_p$, we have the domain $D = [r_\delta(z, t) - r_i]$, with $r_\delta(z, t) = r_0 - \delta(z, t)$, where $\delta(z, t)$ is the local ablated material thickness.

When the external flux varies with the axial coordinate, the resultant shape of the ablation front is a function of location, not only because the local ablated material thickness depends on the magnitude of the local heat flux at that instant, but also due to the variation of v_{eff} with incident heat flux for composites. The rate of material removal in this case is not uniform along the axis, and the ablation front is represented by a function $f(r, z, t) = 0$. If the ablation

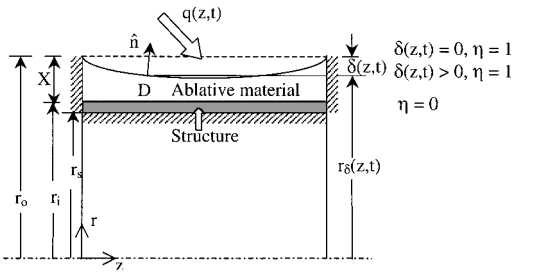

Fig. 3a Schematic of Landau-type[1] transformation for axisymmetric geometry.

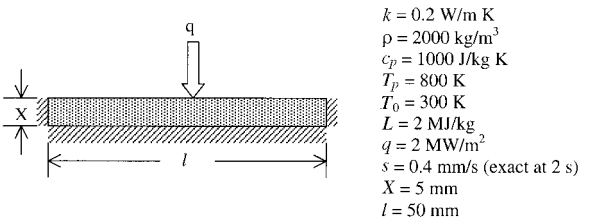

Fig. 3b Example problem with steady-state ablation.

temperature T_p is attained everywhere on the surface, the surface temperature no longer rises, and the recession of ablation front takes place everywhere, but not necessarily uniformly. If the surface temperature has attained T_p even at one location, the heat removal due to the localized ablation affects the temperature field everywhere else. In this case, the surface recession is localized, and only sensible heat transfer takes place at the locations wherever the surface temperature is less than T_p. If the heat flux is no longer applied or decreases after a certain moment at a particular location, the temperature of the moving boundary at that location could descend below T_p, and the front ceases to advance locally, resulting in only sensible heat transfer. If the temperature of the moving boundary descends below T_p everywhere on the surface, only sensible heating of the ablative material takes place throughout, with no recession of the ablation front. When the external flux varies with time in the form of a pulse, it results in a nonlinear local recession rate, and ablation can be a noncontinuous process. All of these cases are included in the following governing equations.

The two-dimensional conduction equation for the ablative material, for domain D

$$\rho c_p \frac{\partial T}{\partial t} = \frac{\partial}{\partial r}\left(k\frac{\partial T}{\partial r}\right) + \frac{k}{r}\frac{\partial T}{\partial r} + \frac{\partial}{\partial z}\left(k\frac{\partial T}{\partial z}\right) \qquad (1)$$

holds good irrespective of the boundary condition whether ablation continues or stops. For the preablation period, domain $D = (r_o - r_i)$ is not a function of axial location. For the ablation period, domain $D = [r_\delta(z, t) - r_i]$ is a function of time as well as location. When the thermophysical properties of the ablative material depend on temperature, the property values are evaluated explicitly, that is, at level l during the first-half time step and at level $l + \frac{1}{2}$ during the second-half time step, thus avoiding an iterative procedure. The maximum temperature rise at the outside surface during the period of one time step is limited to 1 K by the adjustable time step numerical scheme in the present work, thereby limiting the rate of change of property values with time.

The boundary conditions are as follows:

1) The preablation period or ablation front ceases to advance locally. If $T(r, z, t) < T_p$, the local energy balance gives

$$q_{n,\text{net}}|_{z,t} = k\left.\frac{\partial T}{\partial n}\right|_{r = r_\delta, z, t} \qquad (2)$$

on the stationary boundary $f(r, z, t) = 0$, where only sensible heat transfer takes places.

2) The ablation front advances locally. The interface equation for ablation front $f(r, z, t) = 0$ is

$$q_{n,\text{net}}|_{z,t} - k\frac{\partial T}{\partial n}\bigg|_{r=r_\delta,z,t} = -\rho L s_n, \qquad T(r, z, t) = T_p \quad (3)$$

For composites, $L = v_{\text{eff}} c_p (T_p - T_0)$ in the proposed model. The recession rate in the normal direction to the ablating surface s_n is restricted by the complementary conditions $T(r, z, t) < T_p$ and $s_n = 0$ (stationary front) and $T(r, z, t) = T_p$ and $s_n \geq 0$ (moving front).

3) Both ends of the cylinder are assumed to be insulated:

$$\frac{\partial T}{\partial z}\bigg|_{r,t} = 0 \quad \text{at} \quad z = 0 \text{ and } z = l, \quad \text{for} \quad r_i < r < r_\delta \quad (4)$$

4) The boundary conditions for the interior surface are as follows.

a) The insulated boundary condition for the interior surface of the ablative material when the structure is not considered is

$$\frac{\partial T}{\partial r}\bigg|_{r=r_i,z,t} = 0 \quad (5)$$

b) When the ablative material is bonded to a cylindrical structure, the energy balance at the interface without considering the contact resistance is

$$k\frac{\partial T}{\partial n}\bigg|_{r=r_i,z,t} = k_s\frac{\partial T}{\partial r}\bigg|_{r=r_i,z,t} \quad (6a)$$

For the interior surface of the cylindrical structure, an insulated boundary condition is assumed:

$$\frac{\partial T}{\partial r}\bigg|_{r=r_s,z,t} = 0 \quad (6b)$$

The mathematical statement of the problem is completed by the initial conditions:

$$T(r, z, 0) = T_0, \qquad f(r, z, 0) = r_o \quad (7)$$

Equation (3) is the usual energy balance at the interface for moving boundary problems referred to as the Stefan condition. The boundary condition in this form is not suitable for a numerical solution; hence, Eq. (3) is expressed in the more convenient form, following Patel,[15] as

$$q_{r,\text{net}}|_{z,t} - k\left[1 + \left(\frac{\partial \delta}{\partial z}\right)^2\right]\frac{\partial T}{\partial r}\bigg|_{r=r_\delta,z,t} = \rho L\frac{\partial \delta}{\partial t}\bigg|_z \quad (8)$$

in which $\delta(z, t) = r_o - r_\delta(z, t)$ is the local ablated material thickness. This relationship connects explicitly the temperature gradient with derivatives of the moving boundary surface written as $f(r, z, t) = r - r_\delta(z, t) = 0$ or $r = r_\delta(z, t)$.

Coordinate Transformation

It is much simpler to solve a nonlinear differential equation with fixed spatial boundaries numerically rather than solving a linear differential equation in a region with varying spatial boundaries. The boundary immobilization method, which makes the finite difference scheme simple to program is used through a Landau-type transformation,[1] which transforms the coordinate system from (r, z, t) to (η, z, t). The Landau transformation, which was originally developed for moving boundary problems with one-dimensional planar geometries, is extended here to an axisymmetric geometry. It transforms the radial coordinate such that the nondimensional thickness of the remaining ablative material at a particular location (z value) is always unity for all time t as shown schematically in Fig. 3a. Mathematically, the transformation is given by

$$\eta(r, \delta) = \frac{r - r_i}{r_o - r_i - \delta(z, t)} \quad (9)$$

This results in the following: at $r = r_\delta(z, t)$, $\eta = 1$ and at $r = r_i$, $\eta = 0$. $T(r, z, t)$ transformed to $T(\eta, z, t)$ satisfies the following equations.

The two-dimensional conduction equation for the domain D becomes

$$\rho c_p\frac{\partial T}{\partial t} = \frac{k}{(r_o - r_i - \delta)^2}\left[1 + \eta^2\left(\frac{\partial \delta}{\partial z}\right)^2\right]\frac{\partial^2 T}{\partial \eta^2} + \frac{k}{(r_o - r_i - \delta)}\left[\frac{1}{r_i + \eta(r_o - r_i - \delta)} + \frac{2\eta}{(r_o - r_i - \delta)}\left(\frac{\partial \delta}{\partial z}\right)^2 + \eta\frac{\partial^2 \delta}{\partial z^2} - \eta\frac{\rho c_p}{k}\frac{\partial \delta}{\partial t}\right]\frac{\partial T}{\partial \eta} + \frac{2k\eta}{(r_o - r_i - \delta)}\frac{\partial \delta}{\partial z}\frac{\partial^2 T}{\partial \eta \partial z} + k\frac{\partial^2 T}{\partial z^2} + \frac{1}{(r_o - r_i - \delta)^2}\frac{\partial T}{\partial \eta}\frac{\partial k}{\partial \eta} + \left[\frac{\partial T}{\partial z} + \frac{\eta}{(r_o - r_i - \delta)}\frac{\partial \delta}{\partial z}\frac{\partial T}{\partial \eta}\right] \times \left[1 + \frac{\eta}{(r_o - r_i - \delta)}\frac{\partial \delta}{\partial z}\right]\frac{\partial k}{\partial z} \quad (10)$$

The last two terms on the right-hand side of Eq. (10) account for temperature-dependent thermal conductivity and are evaluated explicitly.

The boundary conditions are then as follows:

1) For the preablation period or when ablation front ceases to advance locally, if $T(\eta, z, t) < T_p$ at a location on the interface $r = r_\delta(z, t)$ with $\eta = 1$, then

$$(r_o - r_i - \delta)q_{r,\text{net}}|_{z,t} = k\left[1 + \left(\frac{\partial \delta}{\partial z}\bigg|_t\right)^2\right]\frac{\partial T}{\partial \eta}\bigg|_{\eta=1,z,t} \quad (11)$$

2) When the ablation front advances locally, the interface equation for the local ablation front becomes

$$(r_o - r_i - \delta)q_{r,\text{net}}|_{z,t} - k\left[1 + \left(\frac{\partial \delta}{\partial z}\bigg|_t\right)^2\right]\frac{\partial T}{\partial \eta}\bigg|_{\eta=1,z,t} = \rho L(r_o - r_i - \delta)\frac{\partial \delta}{\partial t}\bigg|_z, \qquad T(\eta, z, t) = T_p \quad (12)$$

on the moving boundary $r = r_\delta(z, t)$ with $\eta = 1$; with complementary conditions $T(\eta, z, t) < T_p$ and $s_n = 0$ and (stationary front) and $T(\eta, z, t) = T_p$ and $s_n \geq 0$ (moving front).

3) The boundary condition at the ends of the cylinder becomes

$$\frac{\partial T}{\partial z}\bigg|_{\eta,t} = -\frac{\eta}{r_o - r_i - \delta(z, t)}\frac{\partial \delta}{\partial z}\frac{\partial T}{\partial \eta}\bigg|_{z,t} \quad \text{at} \quad z = 0 \text{ and } z = l, \quad \text{for} \quad 0 < \eta < 1 \quad (13)$$

4) The boundary condition for the interior surface of the ablative material are as follows:

a) The insulated boundary condition for the ablative material when structure is not present is

$$\frac{\partial T}{\partial \eta}\bigg|_{\eta=0,z,t} = 0 \quad (14)$$

b) When the ablative material is bonded to the structure, at the interface

$$\frac{k}{r_o - r_i - \delta(z, t)}\left[1 + \left(\frac{\partial \delta}{\partial z}\right)^2\right]\frac{\partial T}{\partial n}\bigg|_{\eta=0,z,t} = k_s\frac{\partial T}{\partial r}\bigg|_{r=r_i,z,t} \quad (15a)$$

For the interior surface of the structure

$$\left.\frac{\partial T}{\partial r}\right|_{r=r_s,z,t} = 0 \qquad (15b)$$

Finally, the initial conditions become

$$T(\eta, z, 0) = T_0, \qquad 0 \le \eta \le 1, \qquad r_\delta(z, 0) = r_o \qquad (16)$$

Thus, the problem has been transformed into a region where $0 \le \eta \le 1$, and the ablation front is always at $\eta = 1$ at any location z.

Adjustable Time Step Numerical Scheme

The preceding coupled system of equations is solved iteratively at every time level by a finite difference scheme. The two-dimensional conduction equation is solved with the assumed shape of ablation front $r = r_\delta(z, t)$ and with appropriate local boundary conditions that vary over the surface depending on whether the ablation front advances locally or not. By the use of the temperature field thus obtained, the assumed shape of the ablation front is checked by using the Stefan condition at the ablation front. The iterations are continued until all of the values of δ converge to the desired accuracy (10^{-10}%) before proceeding to the next time level. In the described method, the Stefan condition is solved by a semi-implicit scheme and the two-dimensional conduction equation by an alternating direction implicit (ADI) scheme because both schemes are second-order accurate in both spatial and temporal coordinates and also the system of equations reduces to a tridiagonal matrix form. For the first-half time step, the temperature field is obtained by marching in the η direction and for the second-half time step by marching in the z direction.

The time step used for marching not only affects the temperature field obtained, but also the onset time of ablation. This is especially true when ablation is not a continuous process, thus introducing an error each time ablation begins. To track the onset of ablation accurately, at every time level the system of Eqs. (10) and (11) is solved considering only sensible heating throughout the surface. If the surface temperature thus obtained is less than ablation temperature T_p on the whole surface, then throughout the surface no ablation takes place and the temperature field obtained earlier is retained with no recession of the ablation front ($s = 0$). In this case, a predetermined value of time step is used for marching, subjected to the requirement of numerical stability.

However, if the surface temperature obtained by considering only sensible heating exceeds T_p at any location by a large margin, the time step used for marching is reduced to 90% of the previous value of the time step and the system of equations (10) and (11) is solved again. The time step reduction procedure is continued until the maximum surface temperature is within a specified margin ΔT above the ablation temperature [T_p to ($T_p + \Delta T$)] at the location where incident heat flux is maximum. In this case, ablation continues, which may be either localized or throughout the surface, and hence the system equations (10–16) is solved iteratively subjected to appropriate local boundary conditions that vary over the surface. The heat flux boundary condition is used locally if only sensible heat transfer takes place, and the temperature boundary condition is used when ablation continues at a location. To optimize the number of iterations, the δ values to be assumed for the next time level are obtained by extrapolation, based on values already obtained from previous time levels. The iterations begin with the assumed values $\delta(z, t)^{l+1/2}_{\text{assumed}} = 2\delta(z, t)^{l} - \delta(z, t)^{l-1/2}$ and $\delta(z, t)^{l+1}_{\text{assumed}} = 2\delta(z, t)^{l+1/2} - \delta(z, t)^{l}$ for half time step and one time step levels, respectively.

The margin temperature ΔT used in the adjustable time step procedure is equivalent to the temperature rise at a surface node during the period of one time step, if there were only sensible heating. It was chosen to be 1 K for all calculations based on a convergence study that showed that δ values obtained converged to five decimal places when expressed in milimeters. Thus, the time step for ADI marching is determined automatically by the location on the surface where maximum sensible heating takes place, such that the maximum temperature rise is limited to 1 K per time step. The described procedure of time step determination is repeated at every time level so long as the ablation front advances. The time step so determined not only satisfies the numerical stability criterion but also tracks the onset of ablation accurately when ablation is an intermittent process, taking care of any kind of spatial and temporal variation of the incident heat flux.

Quasi-One-Dimensional Model

To suggest an optimum modeling method, the two-dimensional model has been compared with a quasi-one-dimensional model under different conditions. In the quasi-one-dimensional model, the ablative material is divided into a number of elements in the axial direction, and in each element the temperature is assumed to vary only in the radial direction. The inside surface of the ablative material is assumed to be insulated. For each element, the one-dimensional conduction equation in cylindrical coordinates is solved by a semi-implicit finite difference scheme, subjected to either the sensible heating boundary condition or the Stefan condition at the surface, depending on whether ablation is taking place or not. Landau-type[1] transformation is used for boundary immobilization, the details of which are given elsewhere.[8] The number of divisions to be made in the axial direction depends on the spatial variation of the incident heat flux and is decided based on a convergence study on the resultant shape of the ablation front.

Results and Discussion

Validation

Unfortunately, for problems in cylindrical geometry, a two-dimensional solution is not available in the literature. Consequently, the two-dimensional analysis has been compared with one-dimensional ablation, when both ends of a finite length cylinder are insulated and a constant heat flux is applied to a relatively low thermal conductivity ablative material. One-dimensional ablation analyses in planar and cylindrical geometries in turn are validated against Blackwell and Hogan.[8] For the example problem given in Ref. 8 (the geometry, material properties, and boundary conditions are given in Fig. 3b here), Fig. 4 shows the effect of radial grid size on the recession rate at $t = 2$ s for planar one-dimensional ablation and both one- and two-dimensional ablation in cylindrical geometry. The cylindrical geometry considered is the same as the planar geometry problem with the exception that the radius $r_o = X$,

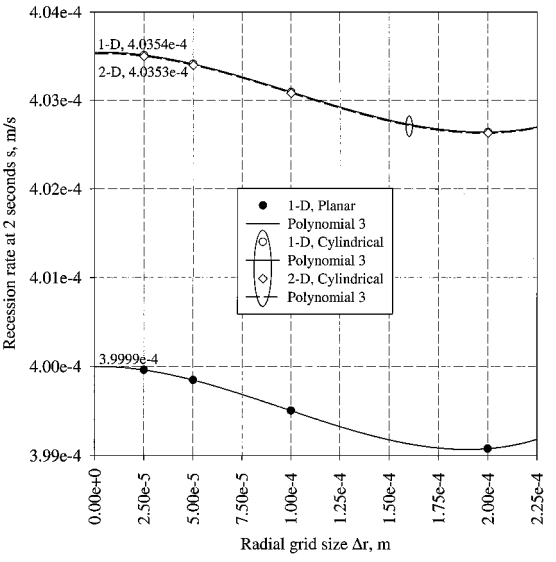

Fig. 4 Effect of variation of radial grid size on surface recession rate.

with $r_i = 0$. The exponential profile given in Ref. 8, namely,

$$\frac{T(r) - T_o}{T_p - T_o} = \exp\left[-\frac{s(r_o - r)}{\alpha}\right]$$

was used as the nonuniform initial temperature. It can be seen that when a polynomial of degree 3 is fitted, the recession rate at 2 s for the planar one-dimensional ablation tends to the exact value of 0.4 mm/s as the grid size tends to zero. Convergence of the one-dimensional ablation in cylindrical geometry follows the same trend, and a third-degree polynomial fit gives a recession rate of 0.40354 mm/s as the grid size tends to zero. Note that the authors of Ref. 8 made use of Richardson's extrapolation to find the recession rate as grid size tends to zero, assuming a quadratic convergence as an approximation (the authors conclude that "we do not know that the convergence is quadratic; however, it should be a reasonable approximation. . ."). The present study shows that the convergence is not quadratic, but the deviation in the recession rate compared with Ref. 8 (which gives a value of 0.40801 mm/s) is small, about 1%. Figure 4 also shows that when one-dimensional conditions are simulated, one- and two-dimensional solutions for ablation in cylindrical geometry match very well. This procedure verifies the accuracy of the present analysis for two-dimensional ablation in cylindrical geometry.

The proposed effective inverse Stefan number procedure for material Avcoat is now validated against experimental results. Reference 12 gives an experimental value for stagnation point surface recession of 7.925 mm at 10 s, for an incident heat flux of 33.61 MW/m^2. By treating the problem as Stefan-type ablation, we obtained corresponding ν_{eff} of 16.96 and the surface recession of 7.913 mm, with an error of 0.15% with respect to the experimental value. This validates the present model against the experimental result for the surface recession rate. Reference 12 gives the details of the experiment in which samples of different materials were tested in an oxidizing environment in the NASA Ames Research Center 60-MW interaction heating facility, for different cold wall heat fluxes. The surface recession was measured by using a template and a height gauge.

Comparison of One-Dimensional Ablation in Planar and Cylindrical Geometries

For the same example problem considered in Fig. 3b, one-dimensional ablation in planar and cylindrical geometries are compared in Fig. 5 for the recession rate and volume rate of ablation for typical values of X/r_i, when X is held fixed at 0.005 m. It can be seen that for planar ablation ($X/r_i = 0$), the ablated material thickness varies almost linearly with time, which results in a constant recession rate of the ablation front. Because the surface area exposed to the heat flux does not vary with time, the volume rate of ablation is also constant in this case. However, in the case of ablation in cylindrical geometry ($X/r_i > 0$) as more and more material is ablated, the surface area exposed to the heat flux, which is a linear function of the outside radius of the virgin material, decreases. Hence, the total heat load on the cylindrical body of the virgin material decreases with time, thereby causing almost a linear fall in the volume rate of ablation, as seen from Fig. 5. Furthermore, as X/r_i decreases, the slope of volume rate of ablation curve decreases gradually until it is zero for planar ablation. Because X is held fixed for all five cases considered, the total heat load increases with decrease in X/r_i, thereby shifting the volume rate of ablation curves upward.

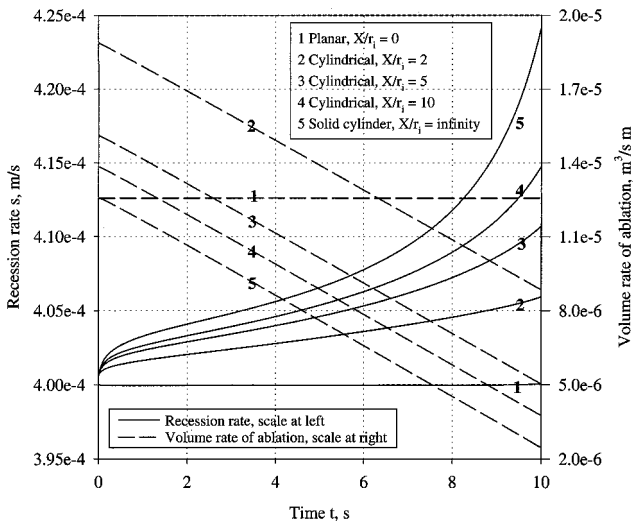

Fig. 5 Comparison of one-dimensional ablation in planar and cylindrical geometries.

However, the recession rate increases with time because it depends on the surface area exposed, incident heat flux, and heat conducted into the material after accounting for latent heat of the ablated material. The curvature effect of the ablating boundary plays an important role because the recession rate is affected by X/r_i. The recession rate at a given instant is maximum for a solid cylinder ($X/r_i = \infty$) and decreases with decreasing X/r_i for hollow cylinders. The recession rate at any instant for a finite X/r_i would lie between the planar and solid cylinder cases. For the same original heat load because the exposed area of the cylinder decreases with time, the ablated material thickness in cylindrical ablation is always larger when compared to the corresponding planar case. This difference in predicted ablated material thicknesses becomes larger and larger as time progresses because the effect of curvature plays an important role when the original virgin material thickness or X/r_i is relatively large. Hence, when ablation takes place over a long period of time, the curvature effect cannot be neglected in ablation modeling, and the planar approximation is not a conservative approach while designing TPS for a cylindrical spacecraft. If ablation were to take place on the inside surface of a hollow cylinder and proceed outward (as in a rocket nozzle), the ablated material thickness at any instant would be smaller when compared to the corresponding planar ablation, and the velocity of ablation front would decrease with time. In this case, even if the curvature effect were neglected the approach would be conservative.

Ablation Modeling in Cylindrical Geometry

To suggest the optimum modeling method under different conditions, quasi-one-dimensional and two-dimensional models are compared for two different ablative materials, namely, Avcoat 5026 H/CG and carbon. The cylindrical geometry with $r_i = 1$ m and $l = 1$ m and with an insulated boundary condition on the inside surface is considered for this comparison. The effect of variation of the proposed ν_{eff} with the incident heat flux for Avcoat is studied. To study the effect of highly conducting metallic structure when the ablative material is bonded to it, a 2-mm-thick aluminum alloy AA2014 ($\rho_s = 2780$ kg/m^3, $c_{p,s} = 963$ J/kg K, and k_s=121 W/m K) with $r_s = 0.998$ m is considered.

Avcoat 5026 H/CG

Ablation of low-thermal-conductivity, 20-mm-thick Avcoat 5026 H/CG is considered. Four cases are studied for comparison, namely, quasi-one-dimensional model, two-dimensional model, two-dimensional model with highly conducting cylindrical structure attached, and two-dimensional model with a constant effective inverse Stefan number. The grid sizes in the radial and axial directions were chosen to be 0.2 and 12.5 mm, respectively, based on a convergence study on the shape of the ablation front and temperature field predictions for a step change in the incident heat flux, which can be considered as the worst-case variation. A sinusoidal variation of the incident heat flux with respect to both axial and temporal coordinates in the form

$$q(z, t) = \{C_1 + C_2 \sin(\pi t/5 - \pi/2)\}\{0.2 + \sin(\pi z/l)\} \qquad (17)$$

with $C_1 = 12.51 \times 10^6$ and $C_2 = 1.16 \times 10^6$ was chosen such that over a period of 20 s it varies from 2.27 to 16.4 MW/m^2 in two cycles, to cover the range for which property data are available.

Figure 6 shows the shape of ablation front and inside surface temperature distribution at 20 s for all four cases considered. It can be

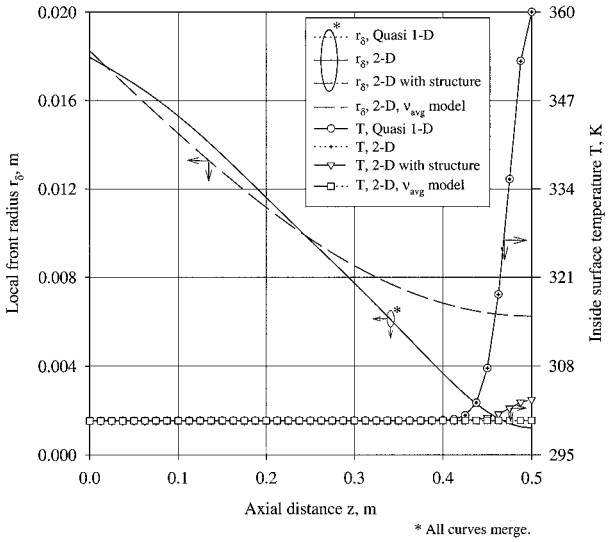

Fig. 6 Shape of ablation front and inside surface temperature distribution, Avcoat.

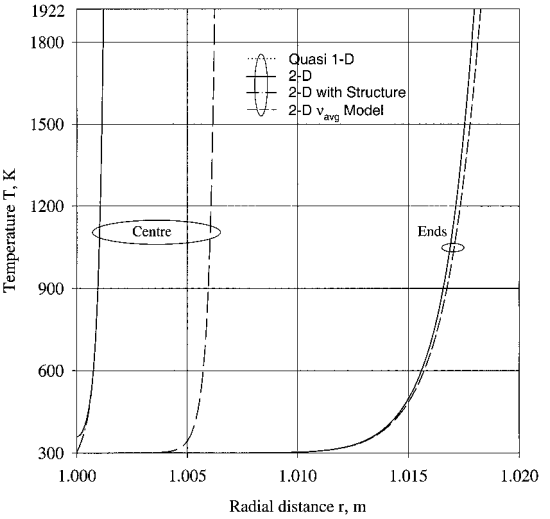

Fig. 7 Temperature profile across Avcoat.

seen that there is no significant difference in the shape of the ablation front predicted by quasi-one-dimensional and two-dimensional models, and also there is no significant effect of the highly conducting cylindrical structure on this (first three cases merge in the scale of Fig. 6). To study the effect of variation of v_{eff} with the incident heat flux, a two-dimensional model with a constant average effective inverse Stefan number $v_{\text{avg}} = 7.844$ was considered. It is evident from Fig. 6 that the v_{avg} model predicts considerably smaller ablated material thickness for higher values of incident heat flux compared to the variable v_{eff} model. The higher the incident heat flux, the larger is this difference because v_{eff} decreases rapidly with increase in incident heat flux as shown in Fig. 2. As a consequence, the v_{avg} model predicts lower temperature for the interior surface of the ablative material or the structure to which the ablative material is bonded because Avcoat is a reasonably good insulator. The presence of a highly conducting structure makes the temperature distribution more uniform in its vicinity because the gradient in the axial direction is only about 3 K compared to 60 K from the center to the end when an insulated boundary condition for the interior surface of an ablative material is assumed. Also, the structure reduces the maximum temperature attained by the interior surface of the ablative material at the end of 20 s, by a large margin of about 57 K. The v_{avg} model predicts no temperature rise at all, and the inside surface of the ablative material remains at the uniform initial temperature of 300 K. Hence, the variation of v_{eff} with the incident heat flux cannot be neglected while designing the TPS of a spacecraft because it does not lead to a conservative approach. The v_{avg} model can be adopted only when the incident heat flux variation with location as well as time is not severe, so that v_{eff} remains relatively constant over the range of interest.

Figure 7 shows the temperature profiles across the ablative material both at the center and ends of the cylinder for all four cases considered at the end of 20 s. It can be seen that there is no significant difference between temperature profiles predicted by the quasi-one-dimensional and two-dimensional models, both at the center as well as the ends of the cylinder. This suggests that for a low thermal conductivity ablative material, even though the incident heat flux variation along the axial direction is severe, the quasi-one-dimensional model is good enough from both ablated material thickness and temperature field prediction point of views so long as ablation takes place everywhere, which need not necessarily be uniform. It can also be observed that even though there is no significant effect of the presence of highly conducting cylindrical structure on the shape of the ablation front, the temperature field is affected in the immediate vicinity at the center. At the end of 20 s, because the temperature of the inside surface at both ends of the cylinder remains at the initial temperature, the effect of the structure cannot be observed here. The temperature profile predicted by v_{avg} model differs altogether because it predicts quite smaller ablated material thickness.

The extrapolation of one-dimensional results while interpreting v_{eff} from H_{eff} data for Avcoat, when the incident heat flux varies with location, is justified by the comparisons between quasi-one-dimensional and two-dimensional models because both models match well as long as ablation is a nonlocalized and continuous process.

Carbon

To study the effect of thermal conductivity of the ablative material, ablation of 50-mm-thick, highly conducting carbon (the temperature-dependent properties are taken from Ref. 9) is analyzed. Three cases are considered for comparison, namely, quasi-one-dimensional model, two-dimensional model, and two-dimensional model with highly conducting cylindrical structure attached. The grid sizes in the radial and axial directions were chosen to be 1.25 and 12.5 mm, respectively, based on a convergence study on the shape of ablation front and temperature field predictions. A sinusoidal variation of the incident heat flux with $C_1 = 18 \times 10^6$ and $C_2 = 8 \times 10^6$ in Eq. (17) is considered such that over a period of 20 s it varies from 2 to 31.2 MW/m^2 in two cycles, representative of entry conditions. It was observed that for carbon, too, there is no significant difference between quasi-one-dimensional and two-dimensional models while predicting the shape of the ablation front, and the presence of highly conducting AA2014 structure, too, has no significant effect on this.

Even though there is no significant difference between quasi-one-dimensional and two-dimensional models while predicting the temperature field in the ablation zone, that is, at the center, the two models differ quite significantly in the nonablation zone, that is, at both ends of the cylinder. This is shown in Fig. 8, in which temperature profiles across the ablative material are plotted both at the center and the ends of the cylinder for all three cases considered (the inset shows the region between $r_s = 0.998$ m and $r = 1.03$ m magnified). It can also be seen that the presence of the highly conducting AA2014 cylindrical structure is felt at locations even far removed from the cylindrical structure because of the high thermal conductivity of carbon. These observations can be clearly visualized from Fig. 9, where isotherms at 20 s are shown for all three cases. The isotherm at 3616 K itself is the shape of the ablation front because ablation has stopped at $t = 18.5$ s. The quasi-one-dimensional model predicts lower temperature at any section in the nonablation zone because the axial conduction of heat from the center (where incident heat flux is maximum) to the ends (where incident heat flux is minimum) is ignored by the quasi-one-dimensional model. It can be seen that the effect of the presence of the highly conducting structure is quite significant everywhere, even in the ablation zone.

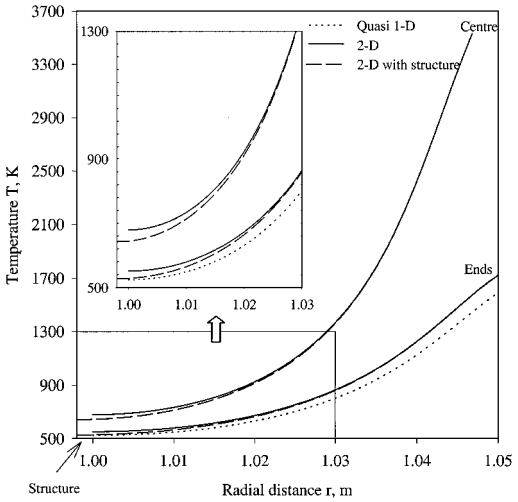

Fig. 8 Temperature profile across carbon; sinusoidal heat flux variation.

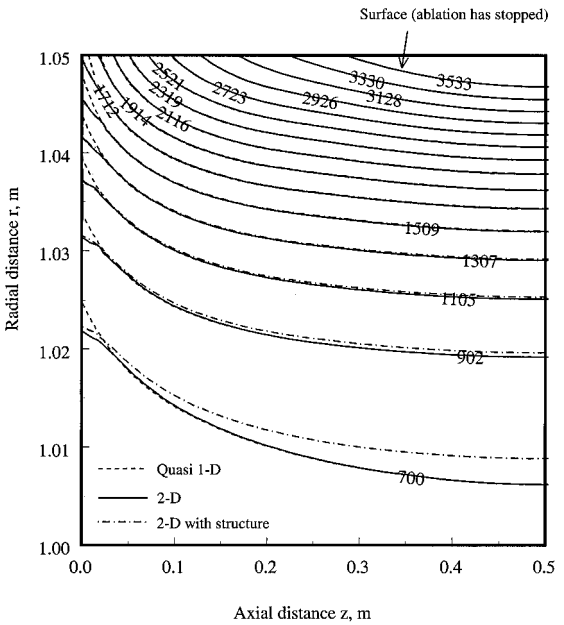

Fig. 9 Isotherms for carbon; sinusoidal heat flux variation.

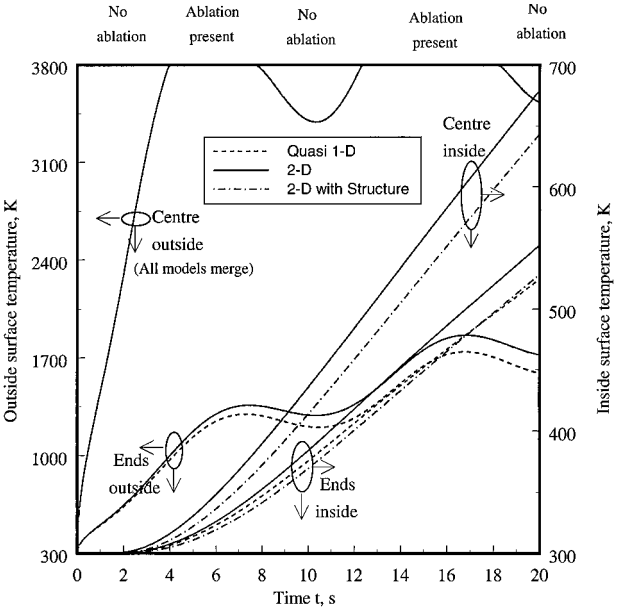

Fig. 10 Surface temperature history for carbon; sinusoidal heat flux variation.

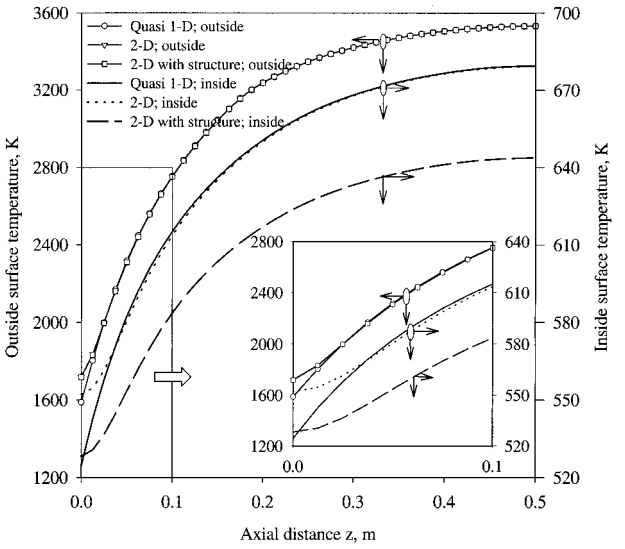

Fig. 11 Surface temperature distribution for carbon; sinusoidal heat flux variation.

Figure 10 shows the temperature histories of the outside and corresponding inside surfaces of carbon, at both the center and ends of the cylinder. Both quasi-one-dimensional and two-dimensional models predict almost the same temperature for the outside surface at the ablation zone, and the presence of a highly conducting structure has no influence on this. Because a sinusoidal variation of incident heat flux with time is considered, even at the center of the cylinder ablation is a noncontinuous process because the surface temperature descends below the ablation temperature of 3800 K twice after it begins at about 3.4 s. Even though the quasi-one-dimensional and two-dimensional models predict almost the same temperature for the inside surface in the ablation zone, the highly conducting structure makes a strong presence because it reduces the temperature level of the interior surface at any instant. It can be seen that, even though ablation front stops to advance between 8.12 and 11.96 s, its effect is not felt at the corresponding interior surface. However, in the nonablation zone, quasi-one-dimensional and two-dimensional models differ quite significantly while predicting the temperatures not only for the inside surface, but also for the outside surface, as shown in Fig. 10. The quasi-one-dimensional model predicts significantly lower temperature for the outside surface, too, compared to the two-dimensional model, as indicated earlier.

Figure 11 shows the temperature distribution of both inside and outside surfaces at 20 s for all three cases considered. As far as the outside surface is concerned, there are no significant differences in the three cases in the ablation zone. However, in the nonablation zone, the quasi-one-dimensional model predicts about 140 K lower temperature compared to the two-dimensional model (the inset shows the nonablation zone magnified). The effect of a highly conducting structure is not felt as far as the outside surface temperature distribution is concerned in both zones. It can be seen that the inside surface temperature distribution differs quite significantly for the two models in the nonablation zone. Also, the structure reduces the temperature gradient along the axis, and it brings down the maximum temperature attained at the end of 20 s at the center, by about 42 K. These observations suggest that as long as ablation takes place everywhere, the ablative material thermal conductivity hardly has any influence either on the shape of ablation front or the temperature field. The requirement for a two-dimensional model arises only when ablation is either noncontinuous or localized or both because the quasi-one-dimensional model is not a conservative approach for temperature field prediction.

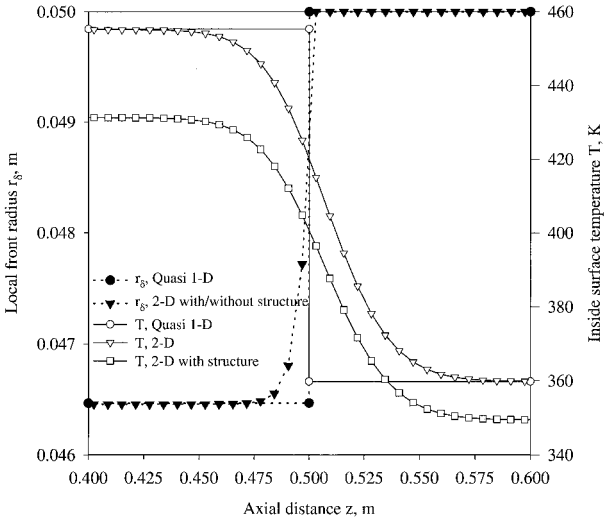

Fig. 12 Shape of ablation front and inside surface temperature distribution, carbon, step change.

Finally a step change in the incident heat flux, 32 MW/m^2 on the first half of the cylinder and 2 MW/m^2 on the second half of the cylinder, is considered, which can be termed as a worst case of heat flux variation. Figure 12 shows the inside surface temperature distribution and the shape of the ablation front at 10 s for the three cases considered. An axial grid size of 12.5 mm is sufficient even for the worst-case variation because both the shape of the ablation front and the inside temperature distribution converge. The effect of two dimensionality can be readily seen because the temperature distributions predicted by quasi-one-dimensional and two-dimensional models differ significantly. Diffusion of heat takes place from the high heat flux zone to the low heat flux zone, thus affecting the inside surface temperature distribution at both zones over a considerable axial distance of about 0.22 m. It can also be seen that the presence of a highly conducting cylindrical structure reduces the temperature level quite significantly in the high heat flux zone (by about 30 K) compared to the low heat flux zone (about 12 K).

Conclusions

Two-dimensional ablation in cylindrical geometry has been considered with temporal and spatial variations of the incident heat flux, which is solved by an adjustable time step ADI scheme, coupled with local boundary immobilization. The effect of curvature is quite significant, and the planar approximation is not a conservative approach. An efficient modeling method has been brought out to account for indirectly the intermediate transformations of the composite materials, through the use of an effective inverse Stefan number. The average effective inverse Stefan number model is not a conservative approach for TPS design, particularly when the incident heat flux varies quite significantly with location. As long as ablation takes place throughout the surface and is continuous, there are no significant differences between the quasi-one-dimensional and two-dimensional models, and the thermal conductivity of the ablative material does not play a significant role. However, if ablation is a localized or intermittent phenomenon or both, the two models differ quite significantly while predicting the temperature field, which is vital, particularly for highly conducting ablative materials. The presence of a highly conducting material structure reduces the temperature gradient in the axial direction in its vicinity, and it has no significant effect on the ablated material thickness.

The major indications on the modeling method from this study are the following:

1) When the effect of structure has to be considered, the quasi-one-dimensional model requires an iterative solution; however, for the two-dimensional model, a standard ADI scheme and tridiagonal matrix algorithm can be used and, hence, computationwise it is advantageous. Modeling is easier for quasi-one-dimensional model compared to two-dimensional model only when the structure is not present. Also the thickness variation of the ablative material in the axial direction can be easily handled by quasi-one-dimensional model if an axially varying thickness TPS is adapted.

2) The quasi-one-dimensional model is accurate for all ablative materials irrespective of thermal conductivity when ablation is a continuous and nonlocalized phenomenon and is suitable when the incident heat flux is not a strong function of location because the computation time increases with the number of elements in the axial direction. The possibility of the localized and noncontinuous ablation necessiates the requirement of a two-dimensional model, particularly for high thermal conductivity materials because the quasi-one-dimensional model does not lead to a conservative estimate for the temperature.

References

[1]Landau, H. G., "Heat Conduction in a Melting Solid," *Quarterly of Applied Mathematics*, Vol. 8, No. 1, 1950, pp. 81–94.

[2]Goodman, T. R., "Heat Balance Integral and Its Application to Problems Involving Phase Change," *Transactions of the American Society of Mechanical Engineers*, Vol. 80, No. 2, 1958, pp. 335–342.

[3]Zien, T. F., "Integral Solutions of Ablation Problems with Time-Dependent Heat Flux," *AIAA Journal*, Vol. 16, No. 12, 1978, pp. 1287–1295.

[4]Biot, M. A., and Agrawal, H. C., "Variational Analysis of Ablation for Variable Properties," *Journal of Heat Transfer*, Vol. 86C, No. 3, 1964, pp. 437–442.

[5]Venkateshan, S. P., and Solaiappan, O., "A General Integral Method for One Dimensional Ablation," *Warme- und Stoffubertragung*, Vol. 25, No. 3, 1990, pp. 141–144.

[6]Ledder, G., "An Integral Equation for the Planar Ablation Problem," *International Journal for Engineering Sciences*, Vol. 35, No. 9, 1997, pp. 819–828.

[7]Petrushevsky, V., and Cohen, S., "Nonlinear Inverse Heat Conduction With a Moving Boundary: Heat Flux and Surface Recession Estimation," *Journal of Heat Transfer*, Vol. 121, No. 3, 1999, pp. 708–711.

[8]Blackwell, B. F., and Hogan, R. E., "One-Dimensional Ablation Using Landau Transformation and Finite Control Volume Procedure," *Journal of Thermophysics and Heat Transfer*, Vol. 8, No. 2, 1994, pp. 282–287.

[9]Hogge, M., and Gerrekens, P., "Two-Dimensional Deforming Finite Element Methods for Surface Ablation," *AIAA Journal*, Vol. 23, No. 3, 1985, pp. 465–471.

[10]Storti, M., "Numerical Modeling of Ablation Phenomena as Two-Phase Stefan Problems," *International Journal of Heat and Mass Transfer*, Vol. 38, No. 15, 1995, pp. 2843–2854.

[11]Hogan, R. E., Blackwell, B. F., and Cochran, R. J., "Application of Moving Grid Control Volume Finite Element Method to Ablation Problems," *Journal of Thermophysics and Heat Transfer*, Vol. 10, No. 2, 1996, pp. 312–319.

[12]Tran, H., Johnson, C., Rasky, D., Hui, F., Hsu, M.-T., Chen, T., Chen, Y. K., Paragas, D., and Kobayashi, L., "Phenolic Impregnated Carbon Ablators (PICA) as Thermal Protection Systems for Discovery Missions," NASA TM-110440, April 1997.

[13]Williams, S. D., Curry, D. M., Dennis, C., and Pham, V. T., "Ablation Analysis of the Shuttle Orbiter Oxidation Protected Reinforced Carbon–Carbon," *Journal of Thermophysics and Heat Transfer*, Vol. 9, No. 3, 1995, pp. 478–485.

[14]TPSX Web Edition, NASA Ames Research Center [online database], URL: http://asm.arc.nasa.gov/cgi-bin/tpsx/unrestrict [cited 15 June 1999].

[15]Patel, P. D., "Interface Conditions in Heat Conduction Problems with Change of Phase," *AIAA Journal*, Vol. 6, No. 12, 1968, p. 2454.